excess of Si. The incidence of balls decreased when metallic solvents, including Si, were deliberately added, and this, coupled with the morphological observations, suggests that the balls were incidental to the 2*H* whisker growth mechanism. In fact, it would appear that nucleation of cubic SiC and subsequent formation of a ball on the tip of a 2*H* crystal very likely stops whisker growth. This is borne out by the observation that the short whiskers usually ended with a ball, whereas the longest whiskers were always free of ball terminations. Thus, the VLS mechanism does not appear to provide an explanation of our observations.

PHYSICAL REVIEW VOLUME 143, NUMBER 2 MARCH 1966

Fundamental Optical Absorption in SnS_2 and $SnSe_2$*

G. Domingo,† R. S. Itoga, and C. R. Kannewurf
Department of Electrical Engineering, Northwestern University, Evanston, Illinois
(Received 12 August 1965; revised manuscript received 10 November 1965)

Optical absorption in single-crystal *n*-type SnS_2 and $SnSe_2$ has been studied at 300°K throughout the wavelength range 0.26 to 6.5 μ. Samples suitable for optical measurements were prepared by various vapor-deposition techniques. The electrical characteristics of the samples used in the absorption measurements were as follows: for $SnSe_2$, conductivity 3.6 $(\Omega\ \text{cm})^{-1}$, electron concentration 10^{18} per cm^3, mobility 27 $\text{cm}^2/\text{V sec}$; and for SnS_2, conductivity 10^{-7} $(\Omega\ \text{cm})^{-1}$. From transmittance and reflectance measurements, the absorption coefficient and index of refraction were determined for light polarized perpendicular to the crystallographic symmetry axis. From an analysis of the data in the high-absorption region, direct-transition band gaps of 1.62 and 2.88 eV were found for $SnSe_2$ and SnS_2, respectively. A threshold for possible indirect phonon-assisted transitions was found to occur at 0.97 eV for $SnSe_2$ and at 2.07 eV for SnS_2. Photoconductivity data for SnS_2 are also presented.

INTRODUCTION

RECENT studies of the various physical properties of the tin chalcogenide system have been chiefly concerned with the $Sn(X)$-type compounds. Very little information is now available concerning the physical properties of the anisotropic compounds of the type $Sn(X)_2$, in particular, for properites of SnS_2 and $SnSe_2$. Mooser and Pearson[1] predicted that $SnSe_2$ would exhibit semiconductor behavior. Busch *et al.*[2] verified this prediction from conductivity, Hall effect, and thermoelectric measurements. Similar results were obtained by Asanabe[3] from conductivity and Hall measurements. Electrical measurements for SnS_2 have not been reported.

Both SnS_2 and $SnSe_2$ belong to the hexagonal-CdI_2-structure type (designated the *C*6 type in *Strukturbericht*). The characteristic layer-type growth of the materials crystallizing in this system has made it possible to prepare excellent single-crystal specimens which have suitable geometry for optical measurements. The other principal compound of the $Sn(X)_2$-type chalcogenides, SnO_2, crystallizes in the tetragonal rutile-type structure. Recent optical studies of SnO_2 have been reported in two papers by Summitt *et al.*[4,5] In view of the limited information available in the literature for SnS_2 and $SnSe_2$, it seemed desirable to study additional properties by optical techniques especially since such measurements have not as yet been reported for these *C*6-type semiconductors.

EXPERIMENTAL

Polycrystalline ingots of SnS_2 and $SnSe_2$ were prepared by melting stoichiometric amounts of the component materials[6] in evacuated quartz tubes. In the case of SnS_2 which has a melting point at approximately 870°C, a 3-mm wall tubing was employed, since at this temperature the vapor pressure of sulfur is over 40 atm. The entire synthesis tube was encased in a stainless steel bomb for further explosion protection. The temperature was increased slowly over a 24-h period to 950°C, held constant for 72 h, and then allowed to slow cool to room temperature. In all preparation trials inspection of the ingot showed some evidence of an incomplete reaction with traces of SnS and unreacted sulfur still present in the tube.

* This research was supported by the Advanced Research Projects Agency of the Department of Defense through the Northwestern University Materials Research Center.
† Present address: Northrup Institute of Technology, Inglewood, California.
[1] E. Mooser and W. B. Pearson, Phys. Rev. **101**, 492 (1956).
[2] G. Busch, C. Frohlich, and F. Hulliger, Helv. Phys. Acta **34**, 359 (1961).
[3] S. Asanabe, J. Phys. Soc. Japan **16**, 1789 (1961).
[4] R. Summitt, J. A. Marley, and N. F. Borrelli, J. Phys. Chem. Solids **25**, 1465 (1964).
[5] R. Summitt and N. F. Borrelli, J. Phys. Chem. Solids **26**, 921 (1965).
[6] Sulfur and selenium were obtained from the American Smelting and Refining Company, purity: 0.99999+; tin from the Consolidated Mining and Smelting Company, of Canada, purity: 0.999999.

Since the melting point of $SnSe_2$ is at 657°C, the selenium vapor pressure was not a reaction problem in this synthesis. The temperature of the synthesis tube was increased over an 8 h period to 730°C, held constant for 20 h, and then slow cooled to room temperature.

To promote single-crystal growth, various vapor-deposition techniques were employed. Vapor transport in evacuated quartz tubes was accomplished by placing the tubes in specially prepared two stage ovens with controlled temperature gradients.[7] The best results for SnS_2 were obtained with the high-temperature side at 880°C and the low-temperature side at 620°C, the corresponding values for $SnSe_2$ being 660°C and 625°C, respectively. The growth habit for both materials was in the form of thin single and polycrystalline platelets generally developing in clusters along the tube walls. The thickness of the single crystals varied from 10 μ to 1 mm with the largest having an effective diameter of 6 mm.

Crystal growth by means of iodine transport as described by Nitsche[8] was also employed. For SnS_2 transport conditions were similar to those given by Nitsche *et al.*[9] except that the high-temperature region of the oven was maintained at 700°C. For $SnSe_2$ temperatures of 500°C at the ingot position and 400°C in the region of crystal growth provided the best temperature gradient. The duration of the growth period was varied from 2 to 72 h in both transport methods. For these materials the crystals obtained from the iodine transport method were generally found to have fewer surface defects and growth irregularities than those obtained from transport without a carrier gas. Efforts to obtain thicker specimens by the Stockbarger method were unsuccessful.

An x-ray analysis confirmed the reported structures of SnS_2 and $SnSe_2$ to be hexagonal $C6$ type.[10,2] The growth orientation of the single-crystal platelets are in planes perpendicular to the hexagonal axis of symmetry. The crystals are easily cleaved in planes parallel to the growth faces.

Conductivity and Hall Effect

Thermal-probe tests indicated all $SnSe_2$ material prepared in the present investigation to be n-type. An average electrical conductivity of 3.6 (ohm cm)$^{-1}$ was found for single-crystal material at 300°K with the direction of current flow normal to the c axis. For the samples used in the absorption measurements a negative Hall coefficient of 7.4 cm^3/C at 300°K was obtained with the magnetic field along the c axis. The average electron concentration was 10^{18}/cm^3, and the Hall mobility was 27 cm^2/V sec which were calculated using $R_H=-3\pi/8en_e$ where R_H is the Hall coefficient. These values are in good agreement with the representative measurements reported by Asanabe[3] for n-type material and also with those reported by Busch *et al.*[2]; however in the Busch work all single-crystal material studied was p-type. All SnS_2 crystals were also found to be n-type with an average conductivity of 10^{-7} (ohm cm)$^{-1}$. Grimm and Nasledov[11] have also prepared both SnS_2 and $SnSe_2$ and found only n-type conduction.

Optical Measurements

Throughout the wavelength range 0.2 to 2.5 μ absorption and reflection measurements were made with a Zeiss *MM* 12 double monochromator with interchangeable optics. The standard Zeiss sources and spectrophotometer detector units were employed. The sample-in–sample-out technique was used to obtain the percent transmission with the samples mounted over various circular apertures ranging in diameter from 3 to 60 mils. For wavelengths greater than 2.5 μ a Hilger monochromator with rock salt optics was used in conjunction with a Nernst glower source and a Schwarz thermopile detector. Data were taken for the most part on a point by point basis for greater accuracy. Over most of the visible and near infrared region the resolution was better than 10 mμ. Reproducibility of the transmission data was to within $\frac{1}{2}$%.

Transmission data were analyzed to obtain the absorption coefficient α using the relation[12]

$$T=\frac{(1-R)^2(1+k^2/n^2)}{e^{\alpha d}-R^2e^{-\alpha d}},$$

where T is the percent transmission, d is the sample thickness, k is the absorption index, n is the index of refraction, and R is the reflectivity: $R=[(n-1)^2+k^2]/[(n+1)^2+k^2]$. The absorption index is related to the absorption coefficient and the wavelength by the expression: $\alpha=4\pi k/\lambda$. Except in the region of very high absorption, the absorption index can be neglected in the numerator of the above transmission equation since $k^2\ll n^2$.

Reflectance data for $SnSe_2$ were taken relative to standard reflecting surfaces whose optical characteristics were known. These surfaces were primarily commercially prepared evaporated films of aluminum. The reflectance characteristics of these films were found to be within 1% agreement with the data presented by Hass[13] for surfaces prepared in a similar manner. As a check on the measurement technique, the method was employed using a polished disk of silicon with known electrical characteristics; the results were in agreement with those quoted in the literature for material with similar char-

[7] G. Domingo, M.S. thesis, Northwestern University, 1965 (unpublished).
[8] R. Nitsche, J. Phys. Chem. Solids **17**, 163 (1960).
[9] R. Nitsche, H. U. Bolsterli, and M. Lichtensteiger, J. Phys. Chem. Solids **21**, 199 (1961).
[10] I. Oftedal, Norsk Geol. Tidsskr. **9**, 225 (1926).
[11] V. R. Grimm and D. N. Nasledov, Zh. Tekhn. Fiz. **26**, 707 (1956) [English transl.: Soviet Phys.—Tech. Phys. **1**, 687 (1957)].
[12] H. Y. Fan, Rept. Progr. Phys. **19**, 107 (1956).
[13] G. Hass, J. Opt. Soc. Am. **45**, 945 (1955).

acteristics. Freshly cleaved surfaces of $SnSe_2$ were used for the reflection measurements with no additional polish treatment. The accuracy of the reflectance data was determined to be $\pm 2\%$ throughout the wavelength range of interest.

In the wavelength region where the transmission is appreciable samples of sufficient thickness were selected so that less than 0.1% of the total reflected radiation was from the back surface reflections in the crystal. The reflectivity for SnS_2 was calculated using the values of the index of refraction obtained from the interference fringes in the transmission data of those samples with the better quality surfaces. Interference fringes in the transmission data for $SnSe_2$ were generally less well defined due to various sample imperfections and consequently were not used to obtain the refractive index. Where the index of refraction of SnS_2 becomes more strongly dependent on wavelength near the onset of the fundamental absorption edge, the same procedure, which was used for $SnSe_2$, was employed.

RESULTS

Transmission data were taken over the wavelength range from 0.26 to 6 μ with all incident radiation along

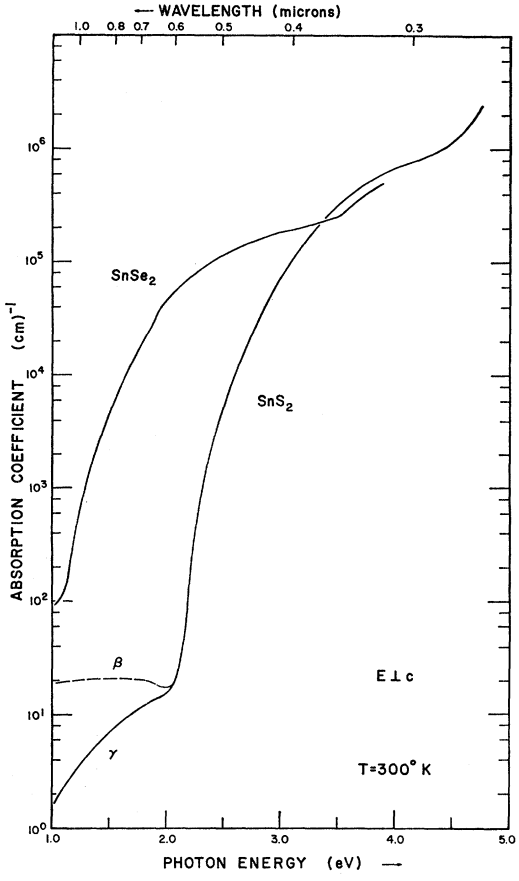

FIG. 1. Absorption coefficient versus photon energy for the fundamental absorption edge in both $SnSe_2$ and SnS_2.

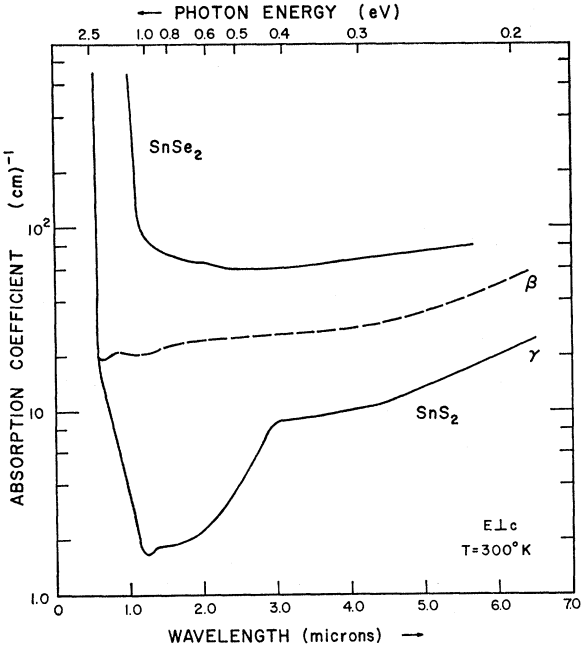

FIG. 2. Absorption coefficient versus wavelength for both materials on the high-transmission side of the fundamental edge. The β and γ branches represent the typical behavior in this region exhibited by various types of SnS_2 crystals.

the hexagonal axis of symmetry ($E \perp c$). Figure 1 shows the dependence of the absorption coefficient on photon energy in the high-absorption region for both single-crystal SnS_2 and $SnSe_2$ at 300°K. These curves are the result of processing transmission data from nearly a hundred samples of various thicknesses. The curves are drawn as continuous since the individual data points would not be resolved on the scale of the drawing. Individual sample thicknesses were measured for all samples with $d > 12$ μ. For $SnSe_2$ sample thickness varied from 0.13 μ in the high-absorption region to 200 μ in the low-absorption region. The corresponding values for SnS_2 were 0.01 to 400 μ. Many samples with a thickness less than 2.5 μ were obtained by cleaving. Most $SnSe_2$ cleaved fragments were not self-supporting and had to be left attached to the cleaving tape for transmission measurements. All SnS_2 samples were self-supporting on the transmission apertures. In the high-absorption region where sample thickness could not be measured, the transmission data were normalized to the established portion of the absorption curve. For SnS_2 with values of α exceeding 10^5 cm^{-1} the absorption index could not be neglected in the numerator of the transmission equation in calculating the absorption coefficient.

In Fig. 2 the variation of absorption coefficient with wavelength is shown on the long-wavelength side of the fundamental edge. In both Figs. 1 and 2 the low-absorption region of the SnS_2 data is divided into two branches labeled β and γ, respectively. The β branch is typical of the behavior of grown single crystals of ap-

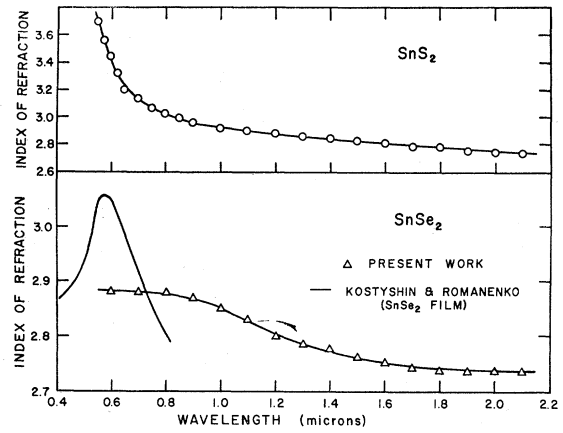

FIG. 3. The index of refraction versus wavelength for both materials. Data from Kostyshin and Romanenko (see Ref. 14) are presented for comparison in the $SnSe_2$ plot.

proximately 100 μ in thickness, which are of sufficient thickness that the interference pattern was not resolved. The γ branch shows a rather unusually high transmission region throughout the wavelength interval 1 to 3 μ. Samples showing this behavior were cleaved single-crystal sections from ingot material with thicknesses generally greater than 300 μ. All microscopic and x-ray examination of these samples showed nothing unusual in their composition and no evidence of internal voids. Beyond 3 μ there were no pronounced differences in the wavelength dependence of the absorption coefficient between samples of types β and γ. The fundamental absorption edge for both SnS_2 and $SnSe_2$ was found to shift toward shorter wavelengths as the sample temperature was lowered to 77°K.

The index of refraction for $SnSe_2$ was computed from the reflectivity data; the results are shown in Fig. 3 and compared with those of Kostyshin and Romanenko.[14] Their samples were evaporated film-type layers. Since efforts to produce such films in the present investigation for photoconductivity work were unsuccessful because of the partial decomposition to free selenium and SnSe, it is proposed that the somewhat higher value for the refractive index at 0.6 μ may be due to the possible heterogeneous composition of the film-type samples. Refractive index data in Fig. 3 for SnS_2 were obtained primarily from the interference fringe pattern in the transmission data for wavelengths greater than 0.8 μ.

Photoconductivity

Both grown and cleaved single-crystal samples of SnS_2 showed a photoconductive response. Samples were mounted at the exit slit of the monochromator with the entire sample being illuminated. Figure 4 shows the photocurrent for a typical sample normalized to a peak response of unity with all incident radiation along the c axis. A 5-V potential difference was applied to the crystal and all current measurements were made with a Keithley 610B electrometer. The dark conductivity of the particular sample shown in Fig. 4 was 3×10^{-8} $(\Omega\ \text{cm})^{-1}$. The peak response is at 0.53 μ. Coblentz[15] attributed the change in resistance of SnS_2 pressed-powder-type samples to a temperature rise rather than to a photoconductive effect. His rise and decay times were in the order of several minutes. The response reported here is photoconductive in nature with a rise time much less than 1 sec and a decay to 5% of the peak response in less than 10 sec at room temperature. Single crystals of $SnSe_2$ showed no measurable photoresponse; attempts to prepare high-resistance film-type layers in evacuated cells resulted in various degrees of chemical decomposition.

DISCUSSION

In accordance with the analysis of optical-absorption data discussed by Bardeen *et al.*[16] the region of high absorption was investigated for evidence of either direct-allowed or direct-forbidden transitions. For values of α greater than 10^3 cm^{-1} no region in photon energy greater than 0.1 eV showed any evidence of a fit for either material to the allowed-direct-transition dependence on photon energy, $h\nu$, of $\alpha \propto (h\nu - E_g)^{1/2}/h\nu$, where E_g is the direct-transition band gap. However, as shown in Fig. 5, there appears to be a good fit for forbidden-direct transitions where $\alpha \propto (h\nu - E_g)^{3/2}/h\nu$ for both materials. The extrapolated values of E_g for $SnSe_2$ and SnS_2 are 1.62 and 2.88 eV±0.02 eV, respectively. Above the region of direct transitions both absorption curves show a

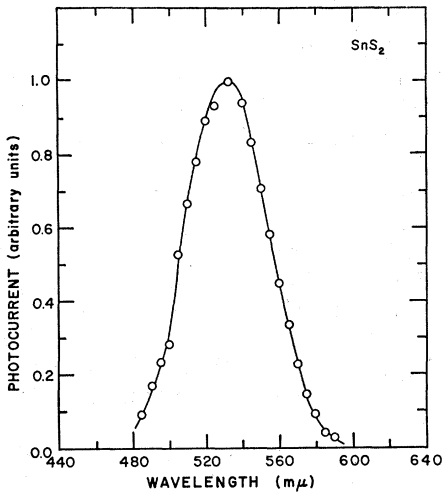

FIG. 4. Photoconductivity of a single crystal of SnS_2 as a function of wavelength at 300°K.

[14] M. T. Kostyshin and P. R. Romanenko, Opt. i Spektroskopiya **12**, 627 (1962) [English transl.: Opt. Spectry. (USSR) **12**, 349 (1962)].

[15] W. W. Coblentz, Sci. Papers Bur. Std. **18**, 585 (1922).

[16] J. Bardeen, F. J. Blatt, and L. H. Hall, *Photoconductivity Conference*, edited by R. Breckenridge, B. Russell, and E. Hahn (John Wiley & Sons, New York, 1956), p. 146.

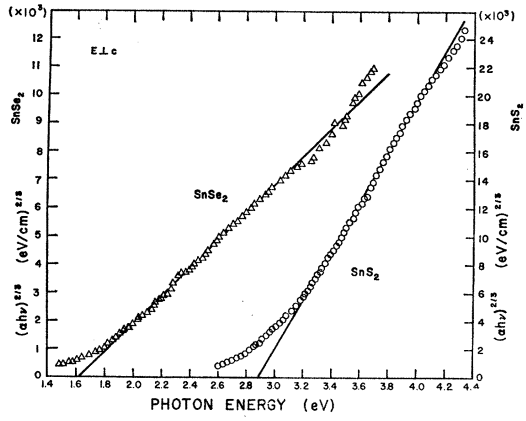

FIG. 5. $(\alpha h\nu)^{2/3}$ versus photon energy for $SnSe_2$ and SnS_2 with both curves extrapolated to the direct band-gap energy value.

definite upward trend which may possibly indicate a change in the nature of the predominate type of absorption mechanism for even higher photon energies. Samples of sufficient thickness with optical quality surfaces were not available to study absorption with the incident radiation polarized parallel to the hexagonal axis.

Below α values of 10^3 cm^{-1} the absorption data were examined for evidence of phonon-assisted indirect transitions. For such transitions $\alpha \propto (h\nu - E_g' \pm E_p)^r/h\nu$ where $r=2$ for allowed-indirect transitions and $r=3$ for forbidden-indirect transitions; E_g' is the indirect-transition band gap and E_p is the absorbed (+) or emitted (−) phonon energy in the transition.[16] Attempts to fit the data to the more theoretically preferred dependence for the allowed-indirect transitions were unsuccessful for both materials. The regions of agreement for the allowed-indirect transitions were so narrow (<0.05 eV) that allowed transitions apparently are not the predominant mechanism in the low-absorption region. A fairly close fit to the energy dependence for the forbidden-indirect transitions was made as shown in Fig. 6 which is in somewhat better agreement for $SnSe_2$ than for SnS_2. The extrapolated energy values are 0.97 and 2.07 eV±0.02 eV for $SnSe_2$ and SnS_2, respectively. Thus the minimum energy band gap E_g' for $SnSe_2$ is $\leq$0.97 eV and $\leq$2.07 eV for SnS_2. The energy of the phonon participating in the transition could not be deduced from the present range of absorption data. Broadening effects at the threshold of the absorption curve imply that possibly more than a single phonon frequency may be involved.

Asanabe[3] states that the variation of electrical conductivity with temperature gives a band gap of approximately 1.0 eV for $SnSe_2$. Busch *et al.*[2] from similar measurements report the value to be 1.0±0.1 eV. Thus the indirect optical band gap of 0.97 eV is in good agreement with the electrical measurements. Electrical conductivity data for SnS_2 have not been reported in the literature. The peak of the photoconductive response at 2.3 eV for SnS_2 lies between the E_g and E_g' values a full 0.5 eV lower than the direct band gap which cannot be satisfactorily explained on the basis of the absorption-curve analysis. The absorption curve exhibits no unusual slope change in the neighborhood of 2.3 eV. In the region of the direct band gap no photoconductive response was detected with the crystals now available.

The absorption data of $SnSe_2$ were examined in the long-wavelength region for free-carrier absorption. Beyond 3 microns α is approximately proportional to $\lambda^{1/2}$ and does not follow any of the established wavelength dependencies for free-carrier absorption.

In view of the absorption analysis we conclude that $SnSe_2$ is a semiconductor with an energy-band configuration such that the lowest minimum in the conduction band occurs at a position in momentum space away from the highest maximum in the valence band since an indirect-transition-type mechanism has been identified for this material. The strong evidence for direct transitions indicates either a higher minimum in the conduction band in the vicinity of the valence-band maximum, or a lower maximum in the valence band in the vicinity of the conduction-band minimum, this transition most likely occurring near the midpoint of the zone.

The general similarities in the features of the absorption analysis between SnS_2 and $SnSe_2$ strongly suggest that these same basic features are present in the energy-band configuration of SnS_2 although the photoconductive response peak is in disagreement with the direct band-gap value. Measurements by Rau[17] on silicon ditelluride, which also belongs to the $C6$ class, indicate a much better agreement between the photoconductive response peak and the direct band-gap value from ab-

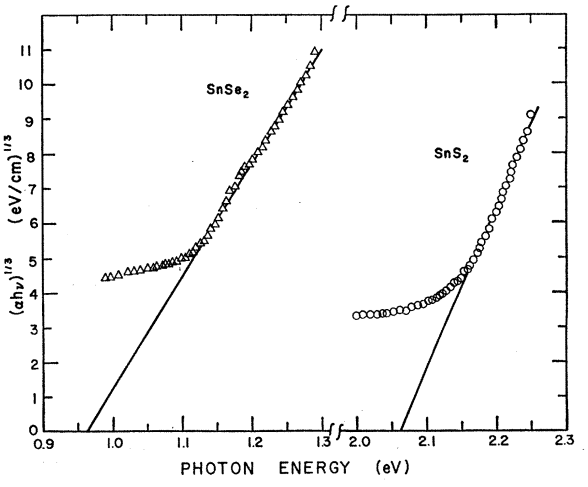

FIG. 6. $(\alpha h\nu)^{1/3}$ versus photon energy for both materials with the curves extrapolated to the threshold energy for indirect phonon-assisted transitions.

[17] J. W. Rau, M.S. thesis, Northwestern University, 1965 (unpublished).

sorption data for the same experimental conditions as described here for SnS_2. More extensive measurements in the infrared wavelength region are being carried out to identify a free-carrier-absorption mechanism in $SnSe_2$ and its correlation to carrier concentration.

Note added in manuscript. A report on the present investigation was recently given by Itoga *et al.*[18] Subsequent to this report, Greenaway and Nitsche[19] have published optical data on several $C6$-type compounds including some absorption data for SnS_2 in the low-absorption region. The general profile of their absorption curve appears to be in good agreement with that obtained in the present investigation. However, in the analysis of the photon energy dependence for the indirect-transition mechanism a preference for a quadratic dependence on energy is shown with more than a single slope indicated. Such structure was not observed in the present investigation. Their mean value for E_g' of 2.21 eV is slightly greater than the corresponding value of 2.07 eV determined here. Absorption data for $\alpha > 10^4$ cm^{-1} were not presented so that a comparison of results in the direct-transition region could not be made.

[18] R. S. Itoga, G. Domingo, and C. R. Kannewurf, Bull. Am. Phys. Soc. **10**, 681 (1965).
[19] D. L. Greenaway and R. Nitsche, J. Phys. Chem. Solids **26**, 1445 (1965).

ACKNOWLEDGMENTS

The authors would like to thank Professor A. W. Ewald for supplying the high-purity tin used in the crystal synthesis and Professor M. E. Brodwin for the use of his magnetic-field equipment.

PHYSICAL REVIEW VOLUME 143, NUMBER 2 MARCH 1966

Electric Field Gradient Calculations in Transition-Metal Sesquioxides

J. O. ARTMAN
Departments of Physics and Electrical Engineering, Carnegie Institute of Technology, Pittsburgh, Pennsylvania

(Received 1 September 1965)

We present computations of the electric field gradient at the cation sites in the Cr, Fe, Ti, and V sesquioxides isomorphous to corundum. We include dipolar as well as monopolar contributions. Except for α-Fe_2O_3 we find that the dipolar and the monopolar field-gradient contributions are opposite in sign and roughly of the same order of magnitude. In so far as existing data permit, we have used these tabulations to determine the electric nuclear quadrupole moment (Q) of the odd isotopes. The Q values found here seem to be somewhat larger than the results of others. In the cases of Cr^{53} and V^{51} existing data are such that only $|Q|$ can be determined. Our calculation for Al^{27} has been given previously. In α-Fe_2O_3 the dipolar field-gradient term has the same sense as the monopolar, and is comparatively small. We find $Q(Fe^{57m})$ to be 0.41 b. A recent α-Fe_2O_3 field-gradient calculation which yielded a $Q(Fe^{57m})$ value of 0.277 b is believed to be in error.

INTRODUCTION

WE present in this paper the results of computations of the electric field gradient at the cation sites in a number of transition-metal sesquioxides.[1] Crystallographically, the structures considered (those of Cr, Fe, Ti, and V) are isomorphous to α-Al_2O_3 (corundum). We include the presence in the lattice of point dipoles as well as point monopoles. In view of the nuclear quadrupole data which increasingly are becoming available we believe that such field-gradient evaluations are of current interest. In the cases of Cr^{53} and V^{51} we are able to evaluate only the absolute value of the nuclear quadrupole moment Q; in the case of Fe^{57m} we evaluate both the magnitude and sign. Our previous results for Al^{27} are also listed.

The corundum lattice can be decomposed into a sequence of bipyramids, each consisting of three O^{2-} ions located on the vertices of an equilateral triangle with the trivalent cations disposed above and below.[2] (See Fig. 1.) From symmetry, both the electric field and the electric field gradient at a cation site must lie along the hexagonal (c) axis. The fields at the O sites lie in the basal plane (perpendicular to the c axis) and are directed along the bisectrices of the oxygen triangles.

At a cationic position the field gradient q_X' can be written as the sum

$$q_X' = q_m' + q_{d-X}' p_X + q_{d-O}' p_O, \quad (1)$$

where q_m' is the usual monopolar contribution; q_{d-X}', q_{d-O}' are the normalized contributions from the dipoles at the X and O sites; and p_X, p_O are the values of the induced dipoles at these sites. These p values follow from solution of the equations

$$\begin{aligned} p_X(1-\alpha_X K_1) - p_O(\alpha_X K_2) &= \alpha_X E_X, \\ -p_X(\alpha_O K_3) + p_O(1-\alpha_O K_4) &= \alpha_O E_O, \end{aligned} \quad (2)$$

[1] A preliminary account was given by J. O. Artman and John C. Murphy in Bull. Am. Phys. Soc. **10**, 488 (1965).
[2] J. O. Artman and John C. Murphy, Phys. Rev. **135**, A1622 (1964).